New Electrode Design for GEPI Shot to Test Curved Sample

Gaël LE BLANC
CEA, DAM, GRAMAT, F-46500 Gramat, France
Pierre L'EPLATTENIER, Inaki CALDICHOURY
Livermore Software Technology Corporation, Livermore, CA, USA

Abstract

This study is relative to material behaviour characterization using the GEPI pulsed power device. First, the GEPI device will be briefly described. At the moment, only planar samples can be tested on GEPI. However, it is very attractive to test curved samples to comply with operational requirements. The adaptation of GEPI to curved sample would allow the characterization of material samples directly extracted from operational cylindrical structures. The GEPI performance is mostly based on high-precision electrode manufacturing. The feasibility study is conducted with the help of LS-DYNA® magneto hydrodynamic modelling. The influence of geometrical defects is studied. To insure the success of this kind of test, the gap between electrodes must be tightly controlled. Electrodes must be machined with a tolerance lower than ten microns.

1 Introduction

This study concerns material behavior characterization under dynamic loading. The GEPI [1][2][3][4] device which allows the generation of high magnetic pressure is used to investigate the quasi isentropic or spalling response of materials. A GEPI shot allows applying controlled and reproducible loading on material sample. Furthermore, contrary to classical dynamic test as plate impact, the sample is not always destroyed during GEPI shot. Hence, a post-mortem analysis is possible to evaluate material damage.

At the moment, only planar samples can be tested on GEPI. However, it is very attractive to test curved samples to comply with operational requirements. The adaptation of GEPI to curved sample would allow the characterization of material samples directly extracted from operational cylindrical structures.

First the GEPI device is briefly described. Then, the numerical feasibility study is presented. The GEPI shot success is mostly based on high precision electrode machining. The feasibility study is conducted with the help of LS-DYNA magneto hydrodynamic modeling [5][6] to determine the influence of electrode geometrical defects. The main objectives are: process validation on nominal configuration and definition of acceptable tolerance for electrode machining defects. The results of numerical simulations will be presented from which some conclusions regarding the electrode design can be drawn.

2 GEPI device description

For several years the CEA Gramat has been studying the behavior of materials by means of experimental devices using High Pulsed Powers technologies. Among them, GEPI is a pulsed power generator devoted to ramp wave (quasi isentropic) compression experiments in the 1 GPa

to 100 GPa pressure range. It may also produce non shocked high velocity flyer plates in the 0.1 km/s to 10 km/s velocity range. The basic principle is based on a strong current circulation into electrodes (see Figure 1). This current generates within the electrodes a magnetic pressure wave via the Laplace forces and a strong rise of the temperature (several thousands K) due to Joule effect (see Figure 1) especially for narrow electrode (width lower or equal to 30 mm).

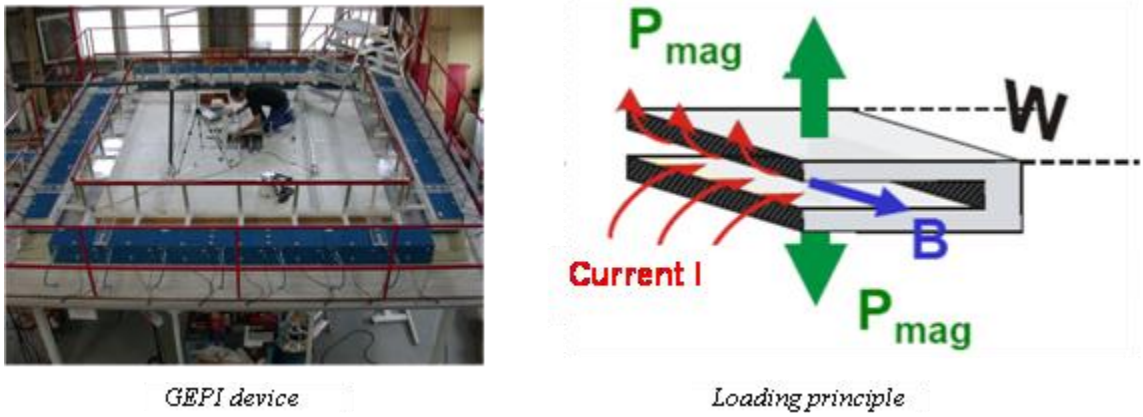

Figure 1: GEPI device and loading principle.

Hence, modeling a GEPI shot requires an Electromagnetism/Mechanical/Thermal 3D solver in order to study all the associated physics. Such a solver is now available in LS-DYNA, and has been used in this work.

3 Computer assisted design of curved electrode for the GEPI device

The first step consists in simulating the nominal configuration to check the pressure loading homogeneity without geometric defect due to for example machining imperfections. In fact, we look for spatial pressure homogeneity at less than 1% deviation in order to insure a quasi one dimensional loading. Then, we focus on geometric defect effect on pressure loading homogeneity. For all models we consider only the terminal part of the electrode.

3.1 Nominal configuration

3.1.1 LS-DYNA modeling

The geometry, mesh and loading are presented on Figure 2.

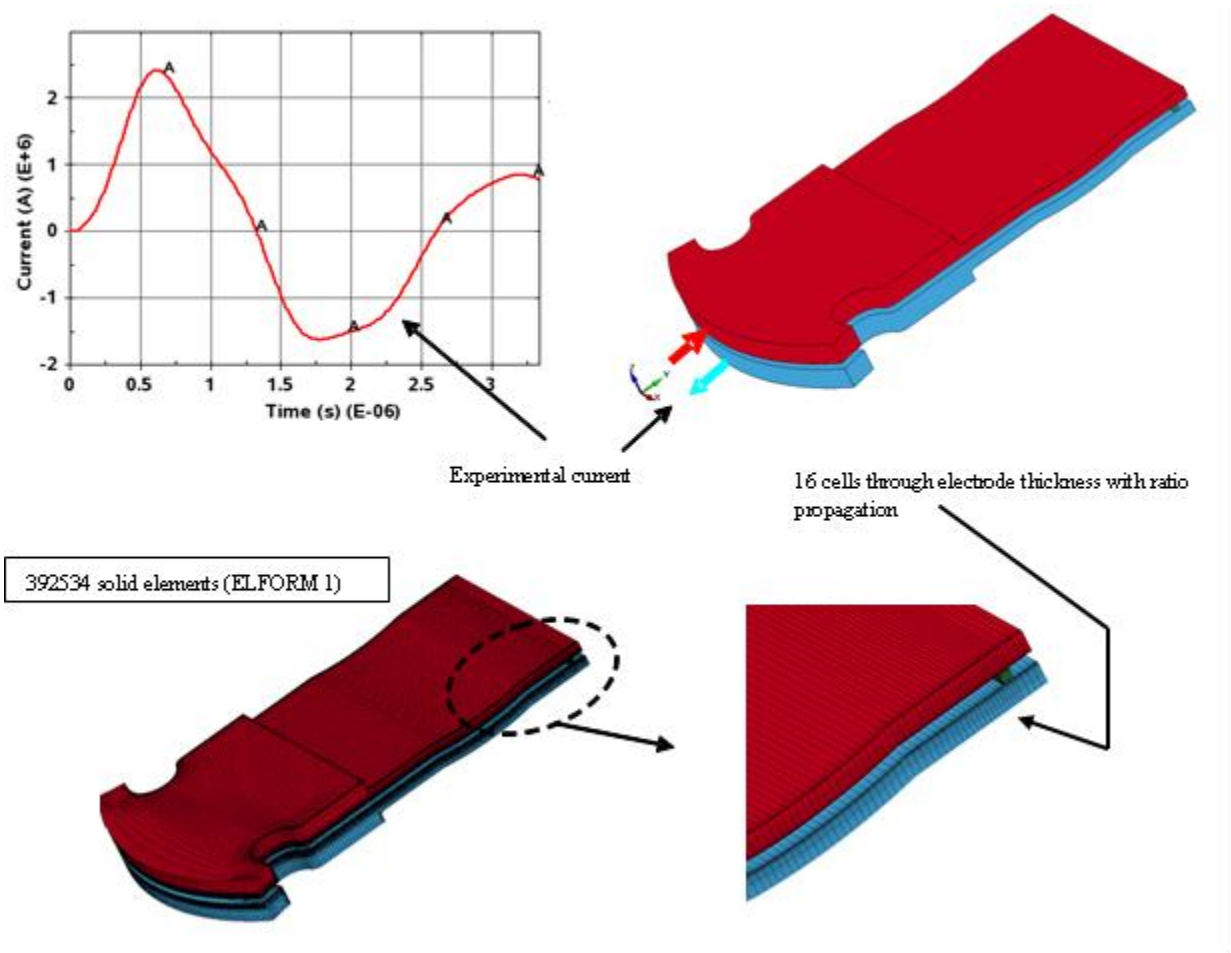

Figure 2 : Geometry, mesh and loading – Nominal configuration.

We use a tridimensional magneto-hydrodynamic modeling with LS-DYNA version 980 (beta version). This modeling takes into account electromagnetic, mechanical ant thermal phenomena. The spatial mesh refinement is driven by the electromagnetic phenomena, especially the magnetic diffusion through the electrode thickness. It is based on the Knoepfel empirical model [7] that defines the skin effect for a strip line crossed by a sinusoidal current.

$$\delta = \left(\mu_0 \cdot \pi \cdot F \cdot \sigma\right)^{-1/2} \quad (1)$$

Where : δ, skin thickness; μ_0, vacuum magnetic permeability; F, current frequency; σ, electrical conductivity.

The application of equation 1 gives a skin thickness close to 0.13 mm. We decide to have two cells in the initial skin depth. Let us also bear in mind that the electrical conductivity decreases with temperature elevation: as the electrode heats up due to Joule effect, the skin depth increases. This mesh refinement may appear insufficient but LS-DYNA uses an element formulation with eight integration points per element. Furthermore this mesh density has been successfully used in previous simulations of GEPI experiments [10][11].

The mechanical behavior of the electrodes is modeled with the Johnson-Cook model [12] associated to the Gruneïsen equation of state [13]. The Burgess resistive [14] and linear thermal models are used. These models are available in LS-DYNA 980 [15][16]. We don't use a multiphase equation of state despite some melting occurring near the gap because its area is

limited and its influence is very weak on the sample loading [11]. It's especially true for the first quarter of loading period.

3.1.2 Results

The analysis focuses mainly on spatial distribution of free surface velocity in the zone where the sample will be stuck on (curl zone). We use velocities for two reasons. First, its distribution is identical to the pressure loading one. Secondly, we can compare easily numerical result to future experimental ones. The velocity history measurements are precisely done during test on multiple points via Doppler Laser Interferometer system [17].

The velocity distribution in two directions, azimuth and transverse, are presented on Figure 3 in terms of discrepancy to the central value. These iso-contour results have been post-processed using user variable option available in LS-PREPOST.

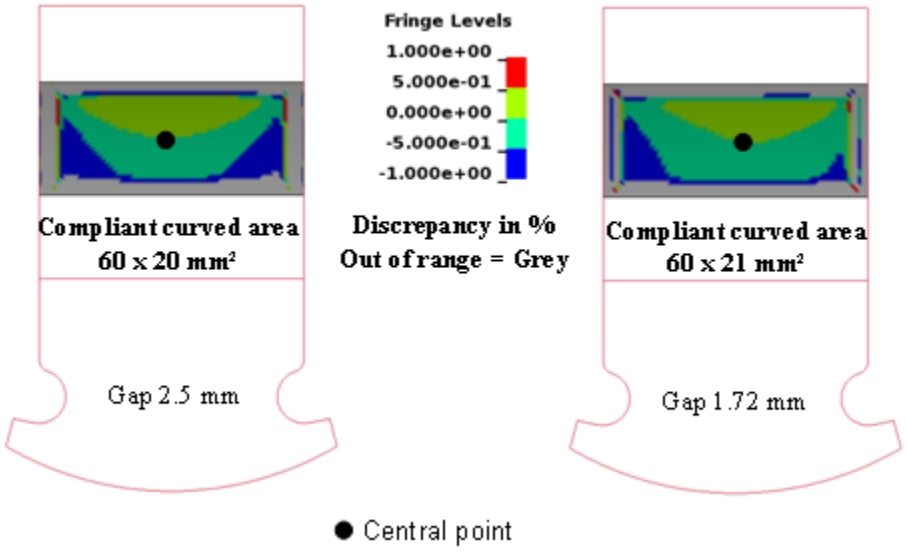

Figure 3 : Pressure loading homogeneity – Deviation to the central value – nominal configuration.

The area where the free surface velocity is homogeneous in space at less than 1% is not dependent on the gap thickness. This area is 60 mm width with an arc of 12° (i.e. 60 mm * 20 mm). Results presented indicate that the feasibility to test curved sample on GEPI device is demonstrated. Nevertheless, we observe a light dissymmetry for a gap of 1.72 mm. This is due to numerical inaccuracy in nodal position after translation and rotation (less than 1µm) during model pre treatment. So, it is very important to study the effect of geometric defects on pressure loading spatial distribution since a quasi perfect homogeneity of the pressure loading is requested.

3.2 Geometrical perturbation effect

Two kind of defects have been analyzed. The first one consists in a gap thickness variation in the transverse direction. The second one consists in geometrical defects due to machining imperfection tolerance.

3.2.1 Gap thickness variation in transverse direction

We study here the influence of gap thickness variation in transverse direction (see Figure 4).

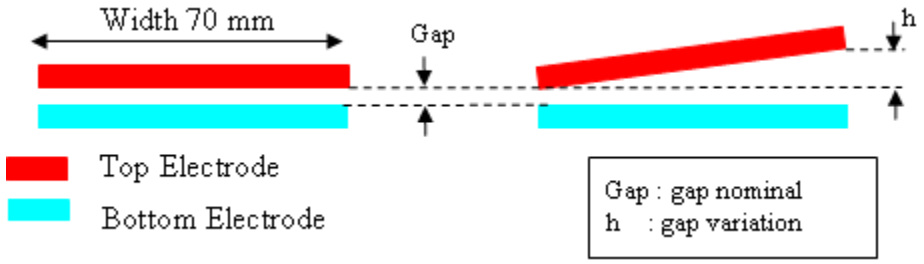

Figure 4 : Linear gap thickness variation in transverse direction.

This kind of defect could occur in case of an assembly defect or in case of a geometrical defect along the width of the electrode extremity that connects the two electrodes and acts as a short-circuit.

Results, in terms of discrepancy to the central value, for two reference gap thicknesses, are presented on Figure *6* and Figure *7* in the transverse and azimuth directions.

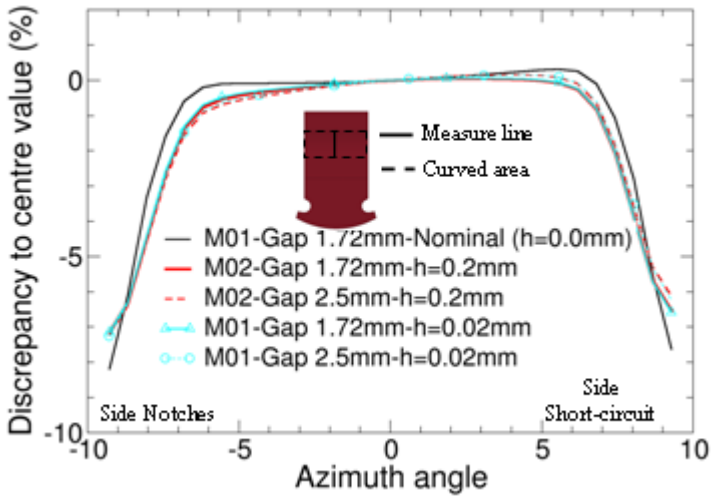

Figure 5 : Pressure loading homogeneity – Deviation from the central value on the curl area – Influence of linear gap thickness variation along azimuth.

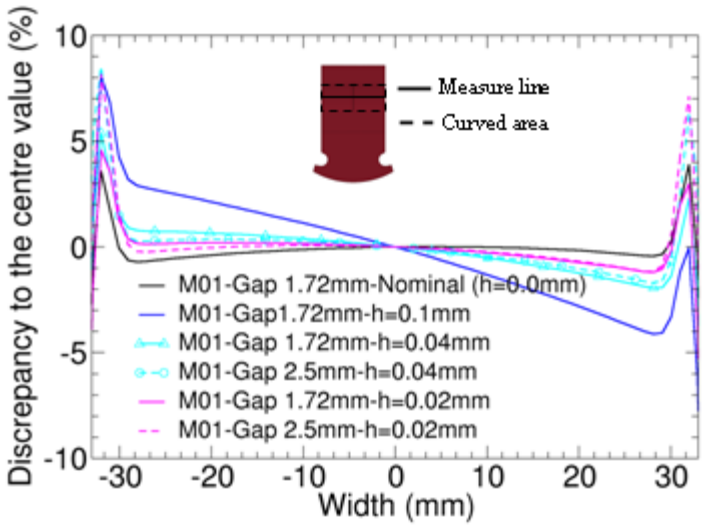

Figure 6 : Pressure loading homogeneity – Deviation from the central value on the curl area – Influence of linear gap thickness variation along width.

The gap variation in transverse direction has almost no effect on spatial distribution in azimuth direction at half-width. Of course, the effect in transverse direction is more marked. Indeed, a discrepancy close to 5% could appear quickly for a gap variation equal to 0.1 mm. If we increase the initial gap thickness, the homogeneity is better. Nevertheless, this is inadequate to obtain the desired homogeneity for pressure loading in order to assure a quasi one-dimensional loading. In fact, the transverse gap variation must be lower than 0.04 mm to assure a quasi one-dimensional loading on the useful area (see Figure *7*).

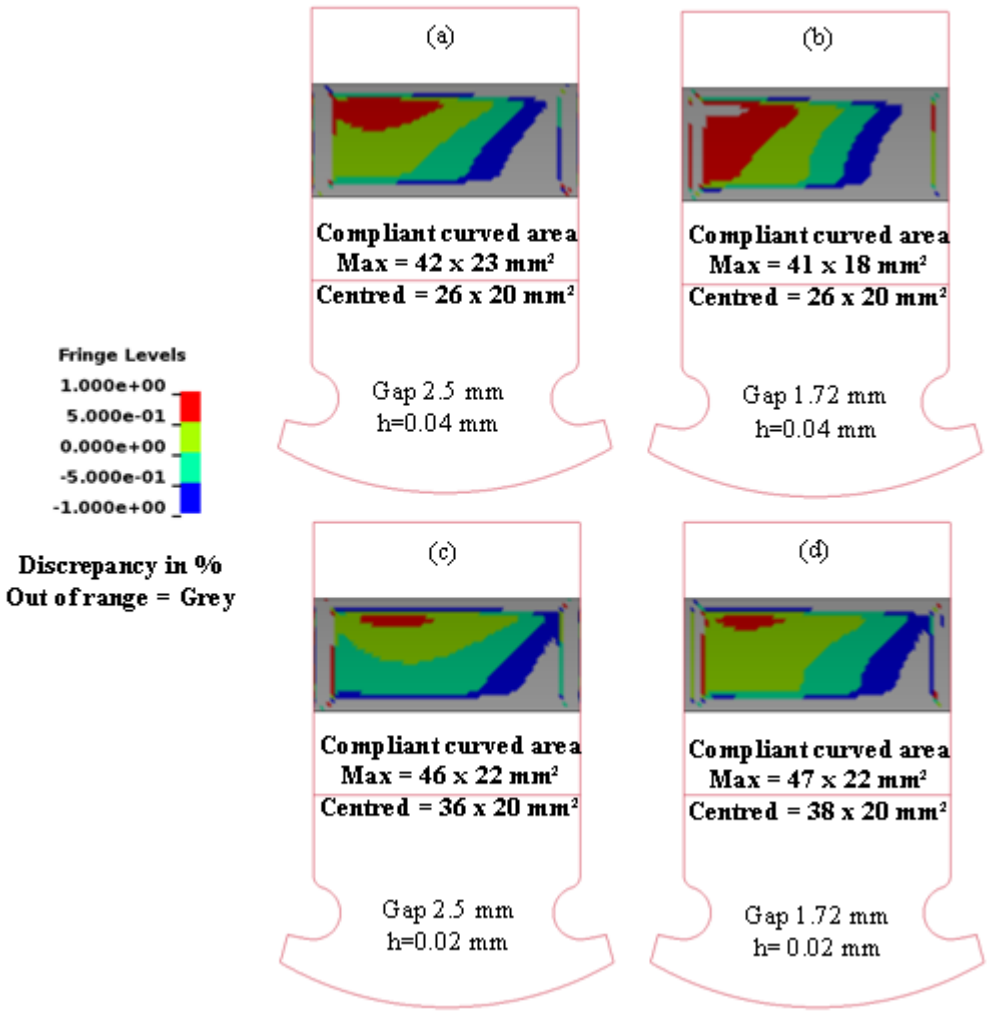

Figure 7 : Pressure loading homogeneity – Deviation to the central value on curl area – Influence of linear gap thickness variation.

A gap variation equals to 0.04 mm involves a homogeneous loading area that is no centered (a and b). So, it is difficult to assure the sample placement in an adequate zone. Consequently, we can only tolerate a gap variation of 0.02 mm (c and d).

The gap variation in longitudinal direction is not studied here for two reasons. Firstly, the assembly process can't generate such defect. Secondly, this kind of defect is less detrimental for the loading homogeneity because it doesn't act on current distribution in transverse direction.

3.2.2 Geometric defect due to machining imperfections

We study the effect of machining related defects in the curved area. In practice, this kind of defect is introduced in LS-DYNA through the perturbation method available in LS-DYNA (*PERTURBATION keyword). The method is based on slight nodes displacement during initialization phase (in radial direction here). We decide to study only the perturbation in gap thickness along the curved surface on both electrodes (see Figure 8).

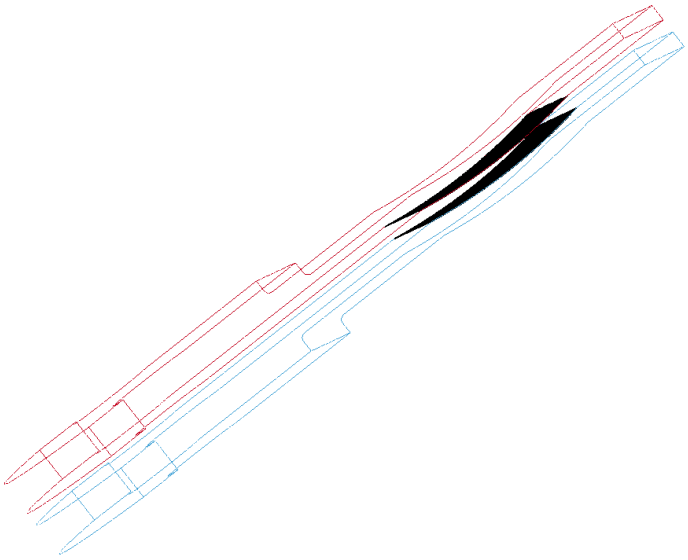

Figure 8 : Perturbation method – Surfaces of application.

Only the radial perturbation is analyzed here in view of cylindrical geometry of each area. The magnitude and spatial distribution of geometrical perturbations are subjected to the following harmonic relation:

$$R = R_{nominal} + \Delta r$$

$$\Delta r = A \cdot \left[\sum_{i=1}^{3} \sin\left(2 \cdot \pi \cdot \frac{x_i + \Delta x_i}{\lambda_i} \right) \right] \qquad (2)$$

With : R, real radius
$R_{nominal}$, nominal radius (theoretical)
Δr, radial perturbation
A, magnitude
x_i, Cartesian coordinates (x, i = 1 ; y, i = 2 ; z, i = 3)
Δx_i, out of phase perturbation
λ_i, wave length along x_i

Different geometrical distributions are analyzed in azimuth and transverse directions.

Azimuth perturbation

The spatial distribution is described Figure 9 for one case. We note that distributions are in opposite phase between bottom and top electrode. This is the case for all perturbations.

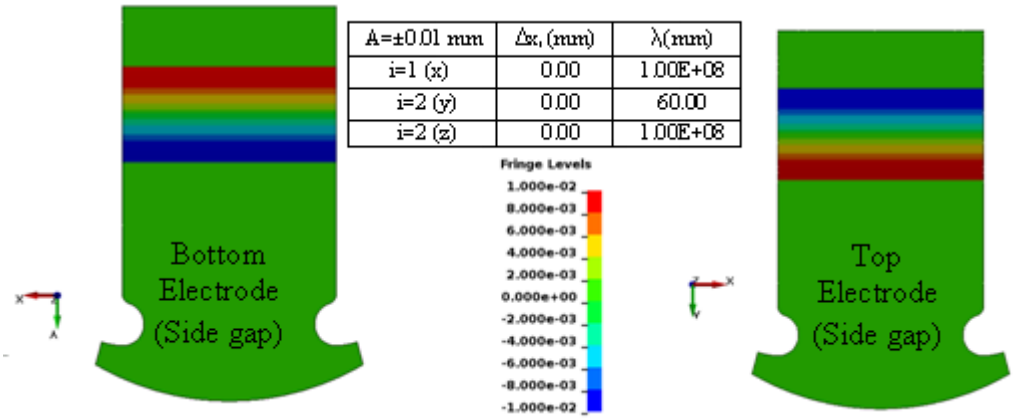

Figure 9 : Example of radial perturbation in azimuth direction.

Different magnitudes of radial perturbation have been tested and the results in terms of deviation to the central value of the work zone are presented Figure 10.

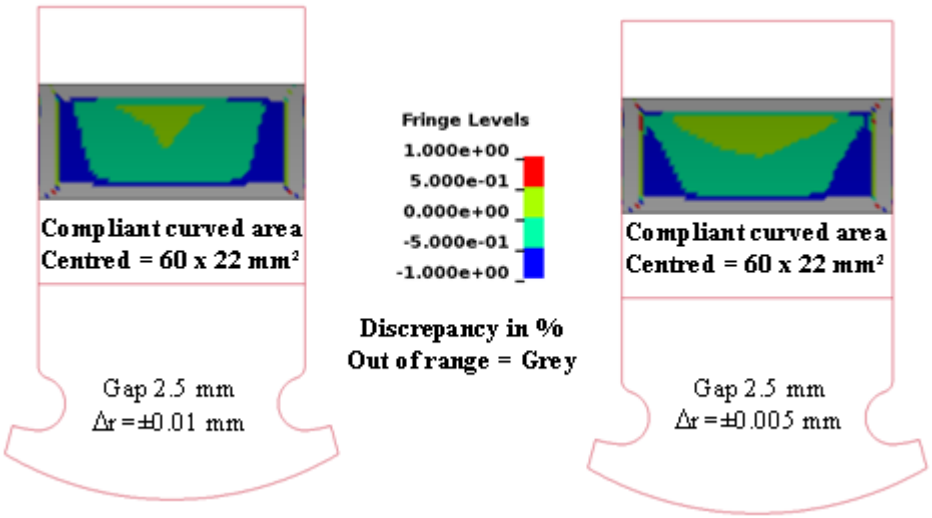

Figure 10 : Pressure loading homogeneity – Influence of radial perturbation along azimuth for two perturbation amplitudes.

The presence of defect along azimuth direction is not critical for the pressure loading homogeneity on the work area even for a 0.04 mm gap variation thickness.

Transverse perturbation

The same method is applied in transverse direction. Three different perturbation distributions are presented on Figure 11.

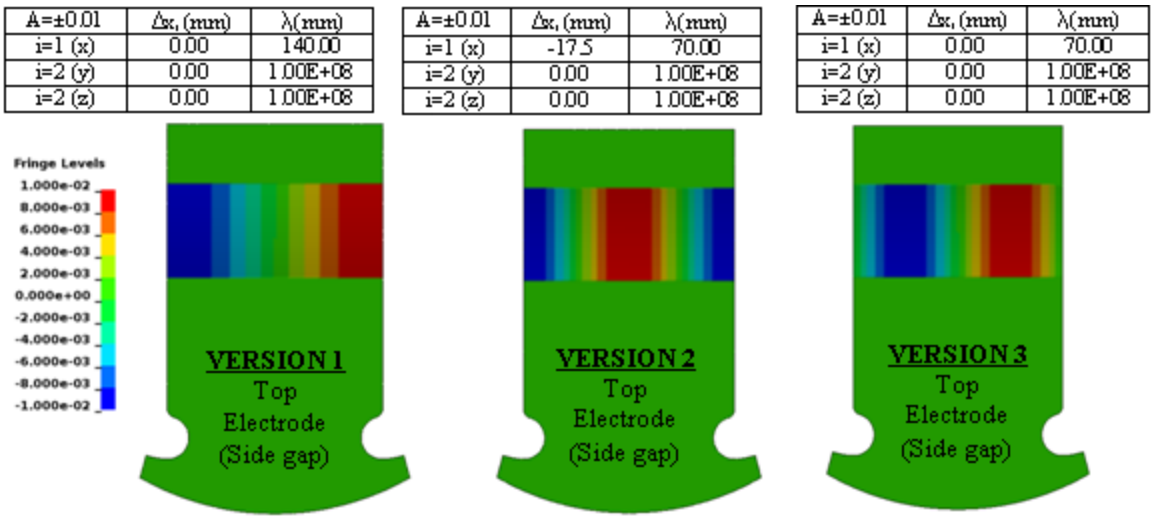

Figure 11 : Transverse perturbation distributions along width.

The pressure loading homogeneity on work area is presented Figure 12 and Figure 13.

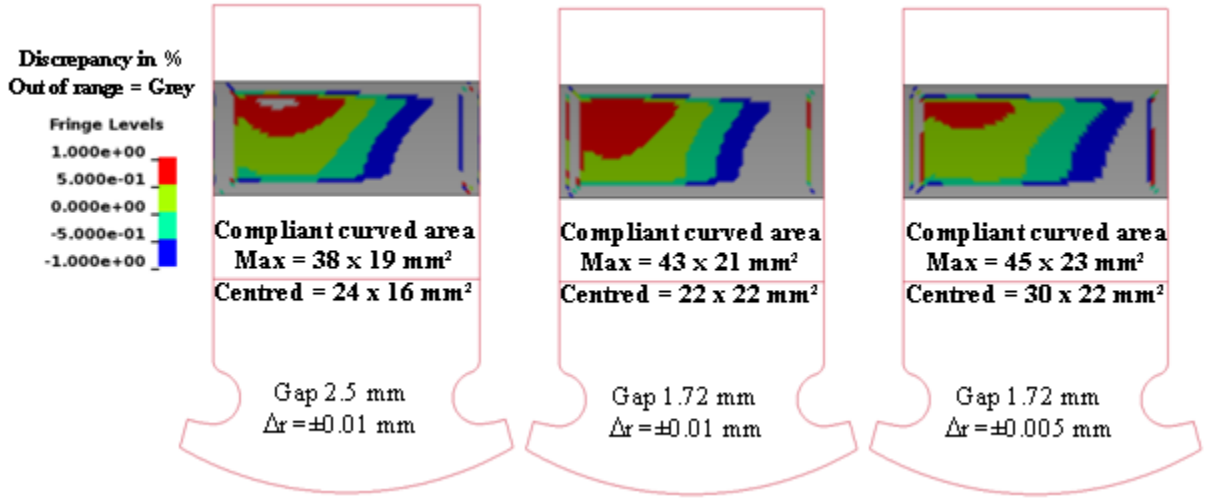

Figure 12 : Pressure loading homogeneity – Deviation to the central value – Influence of radial perturbation along width – VERSION 1.

Firstly, with this kind of defect distribution, the homogeneous discrepancies are close to those observed with the linear gap thickness variation in transverse direction. So, a radial variation of ±0.01mm in opposite phase between top and bottom electrode corresponds to a maximum gap variation in transverse direction equal to 0.04 mm. Nevertheless, a harmonic distribution of defect is more critical than the linear one. Hence, a shape defect greater than 0.02mm is unacceptable for the useful area. So, a reduction of the radial defect magnitude enables an enlargement of the homogeneous area.

Secondly, we analyze the effect of defect distribution wave length and phase on pressure loading distribution. Their actions are noticeable on loading homogeneity. When we reduce the wave length along width (x direction), the current circulates preferably on the left half electrode. This is the worst case for the same radial perturbation magnitude. Nevertheless, loading

homogeneity lower than 4% is conserved on a large area. A long wave length is detrimental to the size of the compliant area.

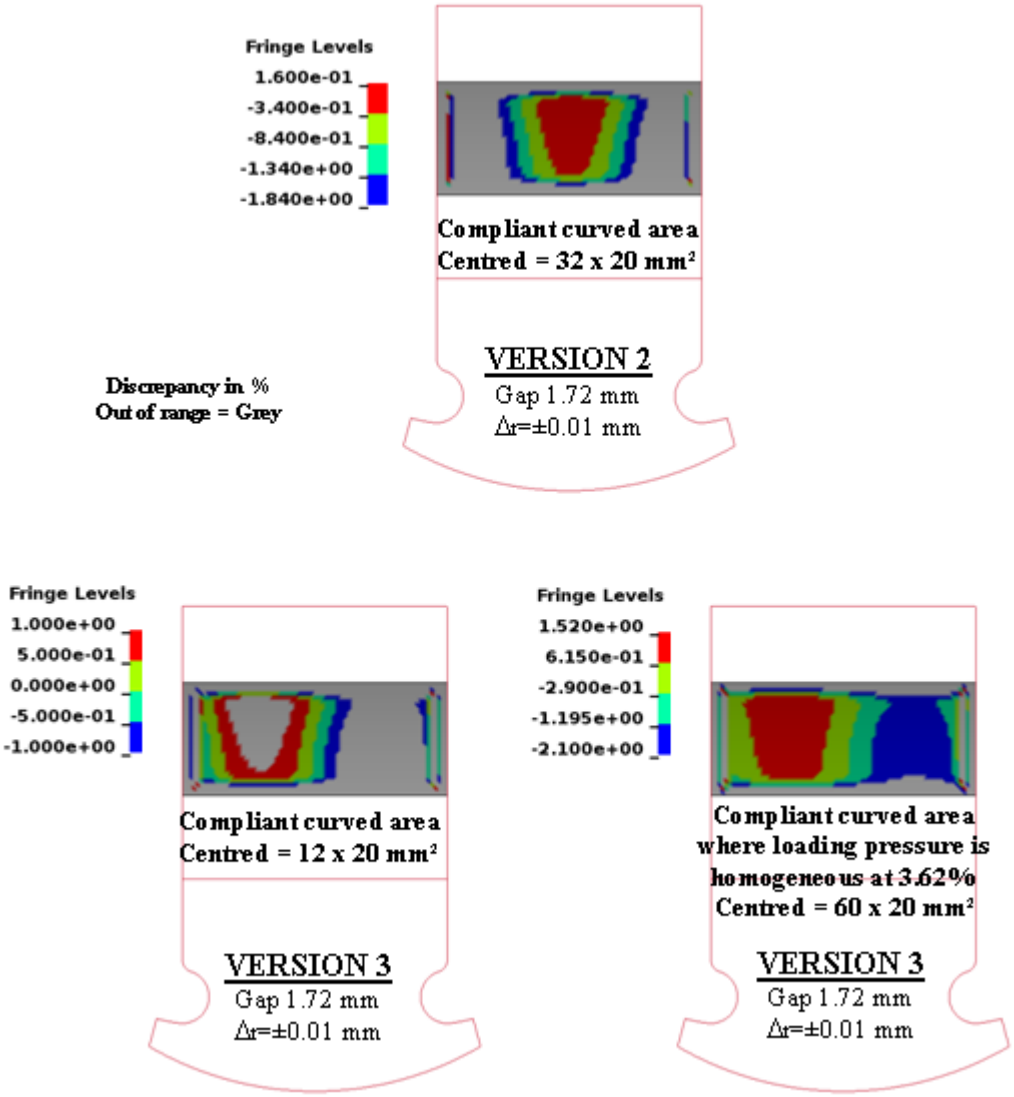

Figure 13 : Pressure loading homogeneity – Deviation to the central value – Influence of radial perturbation along width – VERSIONS 2 & 3.

Perturbation in both directions

The last configuration consists in coupling perturbations in transverse and azimuth direction. An example of such perturbation distribution is presented Figure 14.

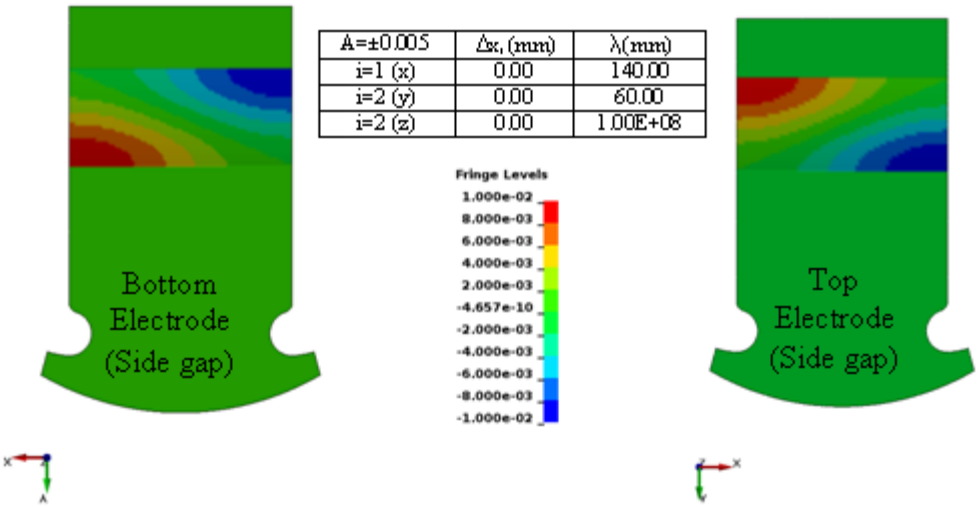

Figure 14 : Radial perturbation distributions along two directions.

The pressure loading homogeneity on useful area is presented Figure 15.

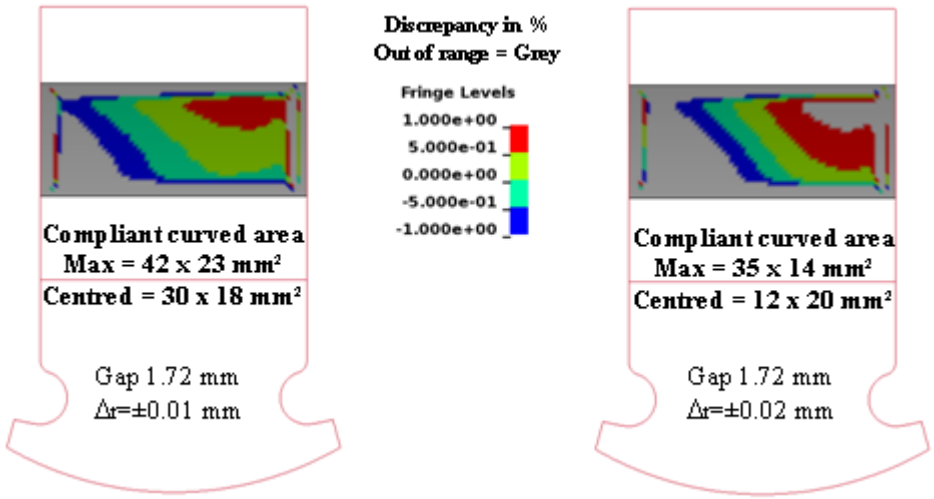

Figure 15 : Pressure loading homogeneity – Deviation to the central value – Influence of radial perturbation in two directions.

The results obtained here confirm the precedent one. The transversal distribution of radial defect is more critical. It is necessary to restrict the amplitude of the defect to a maximum value of 0.02 mm in order to comply with the 1% loading homogeneity requirement.

4 Conclusions

The purpose of this study is a computer assisted design of electrodes for the GEPI device in order to accurately characterize no planar material specimen. Firstly, the feasibility of this kind of test is proved by modeling. Furthermore, modeling results confirm that it is necessary to machine electrode with high precision. Without any defaults on the electrode we can obtain

homogeneous loading on a large area, about 20 mm x 60 mm. Obviously this area decreases when geometrical imperfections appear.

Defect in transversal direction is the worst case because it involves gap thickness variation along electrode width. As a result, the current circulate where the gap is weaker because the inductance is lower in this zone. Consequently, the pressure loading is not homogeneous. Furthermore, spatial defect distribution in opposite phase between top and bottom electrodes must be avoided in order to limit a cumulative effect. Finally, wave length lower than two electrode width must be avoided.

To conclude, curved sample testing on GEPI device is feasible at the cost of a high accuracy in the machining process of the electrodes. Nevertheless, as the configuration is cylindrical, defect is unavoidable in work area. However the loading homogeneity could be guaranteed with a shape defect lower than ± 10 µm in the work area. In this case the homogeneous loading area is greater than 30 mm x 20 mm. In the same way, the assembly process will require a careful monitoring to avoid transverse gap thickness deviation. Thanks to LS-DYNA simulations, we have designed blueprints of the electrodes. The next step will consist in machining the electrodes with compliance to the defect tolerance and testing it on GEPI. Depending on the results, samples with larger arc length may be envisioned. The sample shape defect is usually close to ± 10 µm but the effect on loading homogeneity is minor.

References

[1] "Isentropic compression experiments on the Z accelerator" - Shock Compression of Condensed Matter – J.R. Assay – 1999.

[2] "Dispositif et procédé pour générer des variations contrôlées intenses et brèves de pression magnétique au sein d'un échantillon de matériau solide" - ITHPP - Dépôt de brevet d'invention le 07/07/1999 n° 99.08771 (France) et n° 10/019,943 (USA).

[3] "GEPI : An ICE Generator for Dynamic Material characterization and Hypervelocity Impact" – P. L. Héreil, F. Lassalle and Gilles Avrillaud – Shock Compression of Condensed Matter - 2003.

[4] "GEPI : an ICE generator for dynamic material studies"- P.L. Héreil and G. Avrillaud - Presentation for the 55th Meeting of the Aeroballistic Range Association (ARA), Freiburg, Germany, September 27-October 1, 2004.

[5] "Introduction of an Electromagnetism Module in LS-DYNA for Coupled Mechanical-Thermal-Electromagnetic Simulations" – P. L'Eplattenier, G. Cook, C. Ashcraft, M. Burger, A. Shapiro, G. Daehn and M. Seth – 9th International LS-DYNA Users Conference – 2004.

[6] "Introduction of an Electromagnetism Module in LS-DYNA for Coupled Mechanical-Thermal-Electromagnetic Simulations" – P. L'Eplattenier, G. Cook, C. Ashcraft – 3th International Conference on High Speed Forming – 2008. "LS-DYNA® Keyword User's Manual Version 971" – LSTC – May 2007.

[7] "Pulsed High Magnetic Fields" – H. Knoepfel –NHPC – 1970. "LS-DYNA® Keyword User's Manual Version 971" – LSTC – May 2007.

[8] "Isentropic Compression in a Strip Line, Numerical Simulation and Comparison with GEPI Shot 268" – A. Lefrançois, P. L'Eplattenier and M. Burger – Lawrence Livermore National Laboratory UCRL-TR-219179 – February 2006.

[9] « Etude de l'homogénéité du courant dans la charge par simulations LS-DYNA magnétohydrodynamiques 3D » - G. Le Blanc – ITHPP – 2008.

[10] « Ramp Wave compression in a copper strip line: comparison between MHD numerical simulations (LS-DYNA) and experimental results (GEPI device) » - Le Blanc, Chanal, L'Eplattenier, Avrillaud, Laporte, Vincent – 10TH LS-DYNA international conference – 2008.

[11] « Modelling the dynamic magneto-thermomechanical behaviour of materials using a multi-phase EOS » - Le Blanc, Petit, Chanal, L'Eplattenier, Avrillaud – 7TH LS-DYNA European Conference – 2009.

[12] "A constitutive model and data for Metals Subjected to large Strains, High Strain rates and High Temperatures" – G. R. Johnson, W. H. Cook – Proc 7th Int. symp. on Ballistics, The Hague, The Netherlands – April 1983.

[13] « Equation of state and strength Properties of Selected Materials »– UCRL-MA-106439 - Daniel J. Steinberg – 1996.

[14] "Electrical Resistivity Model of Metal" – T. J. Burgess – 4th international conference on megagauss magnetic-field generation and related topics - July 1986. "LS-DYNA® Keyword User's Manual Version 971" – LSTC – May 2007.

[15] "LS-DYNA® Keyword User's Manual Version 971" – LSTC – May 2007.

[16] "LS-DYNA® Theory Manual" – LSTC compiled by John O. Hallquist – March 2006.

[17] « Innovative laser interferometer's development and metrology for material behaviour studies » – P-Y. Chanal, J. Luc – CEG – 14ème Congrès International de Métrologie – Paris – Juin 2009.